საქართველოს მეცნიერებათა ეროვნული აკადემიის მოამბე, ტ. 18, №1, 2024
BULLETIN OF THE GEORGIAN NATIONAL ACADEMY OF SCIENCES, vol. 18, no. 1, 2024

Materials Science

Impact of Lu_2O_3/Er_2O_3 and $Na_2B_4O_7$ Co-Doping on the Microstructure and Thermoelectric Properties of $CaMnO_3$ Ceramics

Nikoloz Margiani[*], Giorgi Mumladze[*], Andrei Klyndyuk[**], Iamze Kvartskhava[*], Vakhtang Zhghamadze[*], Giorgi Kakhniashvili[*]

[*]*Vladimer Chavchanidze Institute of Cybernetics, Georgian Technical University, Tbilisi, Georgia*
[**]*Department of Physical, Colloid and Analytical Chemistry, Belarusian State Technological University, Minsk, Belarus Republic*

(Presented by Academy Member Tamaz Natriashvili)

The present paper reports on the impact of Lu_2O_3/Er_2O_3 and $Na_2B_4O_7$ co-doping on the microstructure and thermoelectric properties of CaMnO3 ceramics. Reference (undoped) $CaMnO_3$ and dual-doped $Ca_{0.9}Lu_{0.05}[Na_2B_4O_7]_{0.03}MnO_3$, $Ca_{0.9}Er_{0.05}[Na_2B_4O_7]_{0.03}MnO_3$, $Ca_{0.9}Lu_{0.025}Er_{0.025}[Na_2B_4O_7]_{0.03}MnO_3$ thermoelectric materials were prepared by the sol-gel route. The phase purity and microstructure of the samples were examined by X-ray diffraction (XRD) and scanning electron microscopy (SEM) techniques. Electrical and thermal transport characteristics of prepared materials were measured and values of their power factor (*PF*) and figure of merit (*ZT*) were calculated. It was found that the simultaneous incorporation of Lu_2O_3/Er_2O_3 and $Na_2B_4O_7$ dopants into the n-type $CaMnO_3$ system resulted in a marked decrease of electrical resistivity. The sample co-doped with Lu and $Na_2B_4O_7$ possessed the best *PF* and *ZT* values, which are twofold (at 973 K) and fourfold (at 573 K) higher compared to that of the reference $CaMnO_3$. *© 2024 Bull. Georg. Natl. Acad. Sci.*

$CaMnO_3$, co-doping, microstructure, power factor, figure of merit

Negative environmental impacts of global warming have become one of the biggest challenges facing the world today. Therefore, the development of alternative, eco-friendly energy conversion technologies has become increasingly important. Thermoelectric technology can generate clean energy by converting waste heat emitted by various systems directly into profitable electrical power via the Seebeck effect [1]. Due to their high chemical and thermal stability, inexpensiveness, and absence of toxic elements, oxide materials are suitable choices for high-temperature applications [1, 2].

The discoveries of promising thermoelectric properties in *p*-type layered Na_xCoO_2 [3], $Ca_3Co_4O_9$ [4, 5], $Bi_2Sr_2Co_2O_y$ and $Bi_2Ca_2Co_2O_y$ [6, 7] cobaltites gave rise to enormous interest of

research groups all over the world. Typically, a thermoelectric module incorporates both *p*-type and *n*-type materials in which holes and electrons participate in the electrical conduction. However, due to the low heat-to-electricity conversion efficiency in oxide thermoelectric materials, the practical application of oxide-based modules remains challenging [8]. Thermoelectric conversion efficiency of materials are governed by the dimensionless figure-of-merit *ZT*, which is defined in terms of the intrinsic properties of both the *n* and *p* types of materials [1, 9]: $ZT=S^2T/\rho k$, where *S*, *T*, ρ, and *k* are Seebeck coefficient, absolute temperature, electrical resistivity, and total thermal conductivity, respectively. Therefore, the thermoelectric performance rises with increasing of *ZT*. The power factor ($PF=S^2/\rho$), an electrical component of the *ZT* expression, is also used to evaluate the output electrical power [10, 11].

In comparison to *p*-type oxide thermoelectric materials, there are relatively few *n*-type oxide materials, the most promising of which is calcium manganite ($CaMnO_3$) because of its high Seebeck coefficient. However, the electrical resistivity of this compound is too high to be practical [12-17]. Thermoelectric performance of $CaMnO_3$ can be improved by suitable aliovalent doping of various elements at the Ca and/or Mn sites. In particular, numerous investigations have shown that single, dual or triple electron doping of rare earth elements at Ca site is an effective way to enhance the *PF* and *ZT* values of $CaMnO_3$ ceramics [10, 12, 16-24].

In this work, we attempted to optimize thermoelectric performance of $CaMnO_3$ by co-doping with Lu, Er, and $Na_2B_4O_7$. For this purpose, reference and doped $CaMnO_3$ thermoelectric ceramic samples were prepared, and their structural, morphological, and transport properties were studied. Based on the obtained results, the power factor and figure of merit of final products were calculated.

Materials and Methods

Ceramic samples of reference $CaMnO_3$ (N1) and doped $Ca_{0.9}Lu_{0.05}[Na_2B_4O_7]_{0.03}MnO_3$ (N2), $Ca_{0.9}Er_{0.05}[Na_2B_4O_7]_{0.03}MnO_3$ (N3), $Ca_{0.9}Lu_{0.025}Er_{0.025}[Na_2B_4O_7]_{0.03}MnO_3$ (N4) materials were prepared by the sol-gel method using the reagent-grade $CaCO_3$, $Mn(NO_3)_2{\cdot}6H_2O$, Lu_2O_3, Er_2O_3, and $Na_2B_4O_7$ starting materials. To minimize the impact of Na volatilization during sintering [18, 25], an over-stoichiometric quantity of $Na_2B_4O_7$ was chosen in doped samples. Starting materials were dissolved in an aqueous solution of citric acid and ethylene glycol, and a small amount of nitric acid was added. The solutions were stirred using a magnetic stirrer (SMHS-3, Nabitex Scientific GmbH) at 80°C in order to remove the water from the solution and form the gel. The thereby prepared gel was then thermally processed until phase formation began and all organic material had burned away. Then, the obtained powders were calcined at 1173 K, 1223 K, and 1423 K for 15 hours with intermediate manual grindings. The calcined powders were ground, pressed into pellets, and sintered at 1498 K in air for 6.5 h (unlike the [18], without using the sacrificial powders of the same composition), then cooled to room temperature in the furnace. The phase purity and microstructure of the prepared materials were examined using X-ray diffraction (XRD, Dron–3M diffractometer, CuKα–radiation) and scanning electron microscopy (SEM, VEGA TS5130MM) techniques. The temperature dependence of the resistivity $\rho(T)$ and Seebeck coefficient $S(T)$ was determined from room temperature to 973 K with a homemade setup using a KEITHLEY DMM6500 multimeter. Thermal conductivity was measured in the temperature range between 300 and 573 K using the "Hot Disk TPS 500 thermal constants analyzer", coupled with a temperature platform for TPS. Finally, values of *PF* and *ZT* were calculated to evaluate the thermoelectric conversion efficiency of prepared materials.

Results and Discussion

Figure 1 displays XRD patterns of the prepared samples. The observed diffraction peaks are well matched with the standard data for $CaMnO_3$ with the orthorhombic *Pnma* space group (JCPDS card no. 76-1132).

The low-intensity peaks, which are not consistent with the $CaMnO_3$, may be associated with the $CaMn_2O_4$ impurity phase [23, 26]. The higher peak intensity observed for the reference material may be due to a higher degree of crystallinity compared to the doped ones. Doped materials' XRD peaks shift toward lower angles, reflecting unit cell expansion. This increase in cell volume could be attributed to a rise in the Mn^{3+} concentration within the Mn^{4+} matrix [19] because the ionic radius of the Mn^{3+} in the octahedral site (0.645 Å) is larger than that of the Mn^{4+} (0.530 Å) [27].

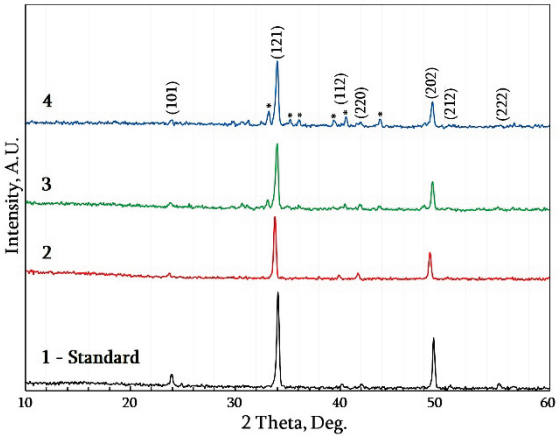

Fig. 1. X-ray diffraction patterns of prepared samples.
1 – Reference $CaMnO_3$;
2 – $Ca_{0.9}Lu_{0.05}[Na_2B_4O_7]_{0.03}MnO_3$;
3 – $Ca_{0.9}Er_{0.05}[Na_2B_4O_7]_{0.03}MnO_3$;
4 – $Ca_{0.9}Lu_{0.025}Er_{0.025}[Na_2B_4O_7]_{0.03}MnO_3$.
* – Secondary phase.

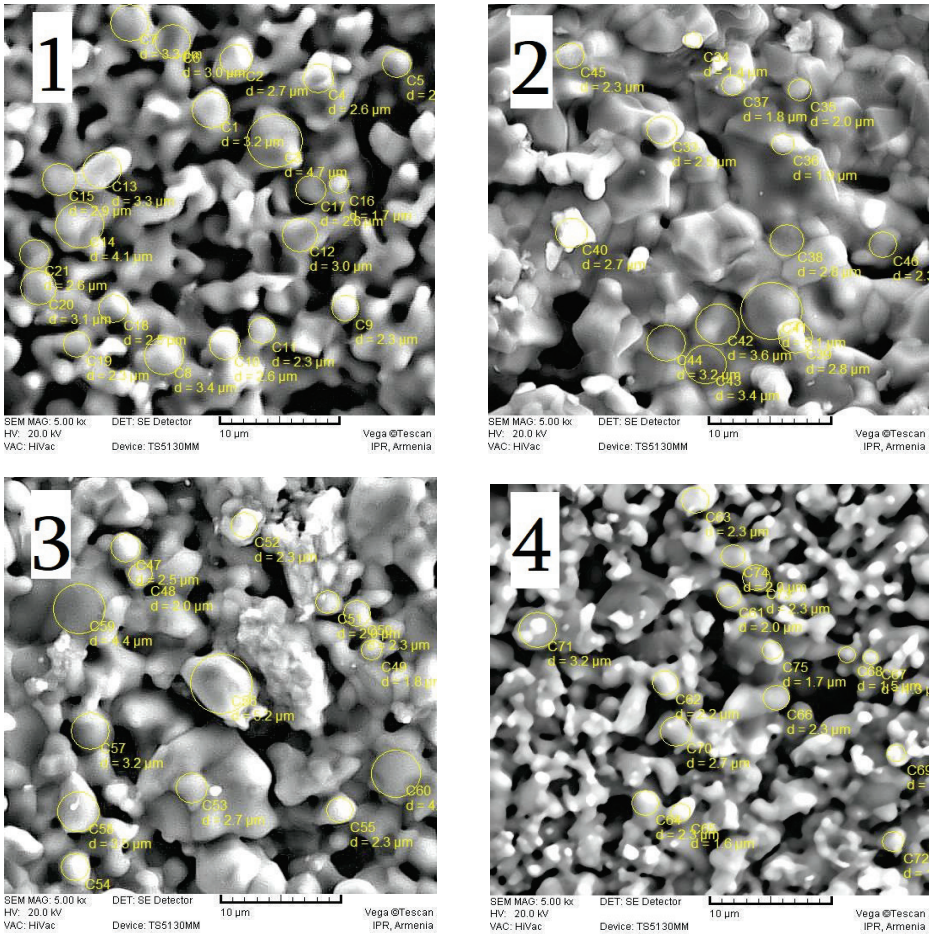

Fig. 2. Surface SEM images with a magnification of 5000×. 1 – Reference $CaMnO_3$; 2 – $Ca_{0.9}Lu_{0.05}[Na_2B_4O_7]_{0.03}MnO_3$; 3 – $Ca_{0.9}Er_{0.05}[Na_2B_4O_7]_{0.03}MnO_3$; 4 – $Ca_{0.9}Lu_{0.025}Er_{0.025}[Na_2B_4O_7]_{0.03}MnO_3$.

Figure 2 shows the surface morphology of prepared samples recorded by SEM. The average grain size for the reference and dual-doped (1÷3) samples ranged between 2.7 and 2.9 μm, while it decreased to 2.0 μm for the triple-doped (4) sample.

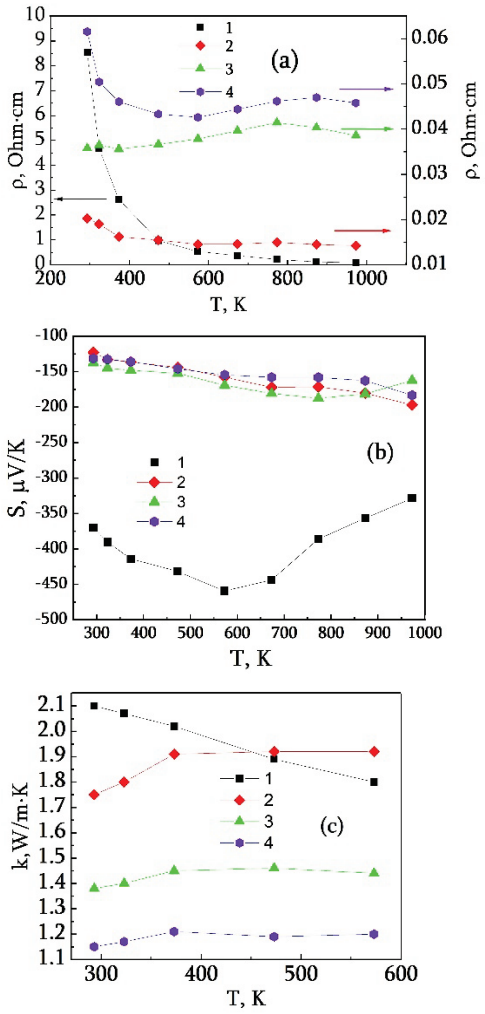

Fig. 3. Temperature dependences of electrical resistivity (a), Seebeck coefficient (b), and thermal conductivity (c). 1 – Reference $CaMnO_3$;
2 – $Ca_{0.9}Lu_{0.05}[Na_2B_4O_7]_{0.03}MnO_3$;
3 – $Ca_{0.9}Er_{0.05}[Na_2B_4O_7]_{0.03}MnO_3$;
4 – $Ca_{0.9}Lu_{0.025}Er_{0.025}[Na_2B_4O_7]_{0.03}MnO_3$.

The samples' mass and geometric dimensions were used to calculate their densities. Density of reference sample, 3.23 g/cm^3, was 70.5% of theoretical value (4.58 g/cm^3) [28]. Co-doping with Lu_2O_3 and $Na_2B_4O_7$ increases the density up to 4.21 g/cm^3 (91.9% of theoretical value). Then, density decreases for $Er_2O_3/Na_2B_4O_7$-doped (3.74 g/cm^3 – 81.7% of theoretical value) and $Er_2O_3/Lu_2O_3/Na_2B_4O_7$-doped (3.31 g/cm^3 – 72.3% of theoretical value) compositions. This implies that the incorporation of $Lu_2O_3/Na_2B_4O_7$ and, to a lesser extent, $Er_2O_3/Na_2B_4O_7$ into $CaMnO_3$ leads to a significant increase in density.

Figure 3 illustrates the temperature dependences of electrical resistivity (ρ), Seebeck coefficient (S), and thermal conductivity (k) of prepared materials.

The value of ρ for the reference sample is 8.5 Ohm·cm at room temperature, which is consistent with the previously published results [29, 30]. Doped samples exhibit substantially reduced resistiveties as compared to reference material. This can be explained by the partial substitution of Lu^{3+}/Er^{3+} for Ca^{2+}, which leads to an increase in carrier concentration and, hence, promotes electron transport. The lower density of the Lu/Er/$Na_2B_4O_7$-doped sample (N4) compared to other doped compounds contributes to increased resistivity. The Seebeck coefficient (Fig. 3(b)) displays negative values for all samples over the entire temperature range, confirming n-type conduction. The reference sample exhibits very large S values, reaching a maximum of -459 μV/K at 573 K, which is consistent with its high resistivity. Due to the rise in carrier concentration, the absolute values of S decrease with doping. The temperature behavior of doped samples' Seebeck coefficient is quite similar in the temperature range between 293 and 973 K, which may be due to the same levels of electron doping. The thermal conductivity of the reference sample (Fig. 3(c)) decreases with increasing temperature, while it is temperature-independent above 375 K for the doped samples. The lowest value of thermal conductivity of the sample (N 4) could be explained by its low density and extra phonon scattering caused by the inhomogeneous microstructure, which is composed of smaller grains and a secondary phase. Fig. 4 shows the temperature dependence of power factor and figure of merit for the reference and doped materials.

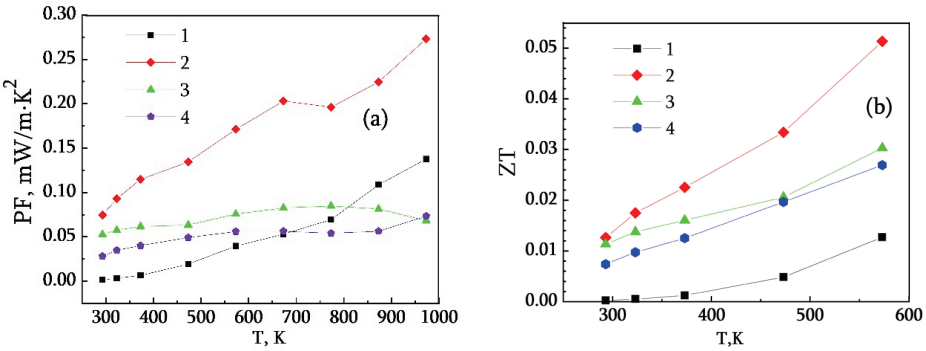

Fig. 4. Temperature dependences of power factor (a) and figure of merit (b). 1 – Reference $CaMnO_3$; 2 – $Ca_{0.9}Lu_{0.05}[Na_2B_4O_7]_{0.03}MnO_3$; 3 – $Ca_{0.9}Er_{0.05}[Na_2B_4O_7]_{0.03}MnO_3$; 4 – $Ca_{0.9}Lu_{0.025}Er_{0.025}[Na_2B_4O_7]_{0.03}MnO_3$.

The highest *PF* value is 0.27 mW/m·K^2 at 973 K for the Lu_2O_3 and $Na_2B_4O_7$ co-doped sample, which is about two times larger than the reference sample. This value is competitive with previously published data on the rare-earth/sodium co-doped $CaMnO_3$ [10, 18]. The simultaneous introduction of Lu_2O_3 and $Na_2B_4O_7$ in the $CaMnO_3$ system led to a 4-fold increase of *ZT* at 573 K.

Conclusions

In this paper, the preliminary results on the impact of Lu_2O_3/Er_2O_3 and $Na_2B_4O_7$ co-doping on the thermoelectric properties of $CaMnO_3$ ceramics are presented. The phase composition and micro-structure of prepared materials were examined using XRD and SEM techniques. Based on the measurements of electrical resistivity, Seebeck coefficient, and thermal conductivity, the *PF* and *ZT* values of the prepared samples were calculated. Co-doping of Lu_2O_3 and $Na_2B_4O_7$ in $CaMnO_3$ system led to a 2-fold increase of power factor and a 4-fold increase of figure of merit at 973 and 573 K, respectively. The *PF* and *ZT* values could be increased further by optimizing the synthesis conditions and doping level.

This research [PHDF-22-442/Influence of borax doping on the thermoelectric performance of layered cobaltites] has been supported by Shota Rustaveli National Science Foundation of Georgia (SRNSFG).

The authors would like to thank Dr. Armen Kuzanyan and Dr. Georgi Badalyan from Institute for Physical Research, Ashtarak, Armenia for the SEM measurements.

მასალათმცოდნეობა

Lu_2O_3/Er_2O_3 და $Na_2B_4O_7$–ით თანადოპირების ზეგავლენა $CaMnO_3$ კერამიკის მიკროსტრუქტურასა და თერმოელექტრულ თვისებებზე

ნ. მარგიანი*, გ. მუმლაძე*, ა. კლინდიუკი**, ი. ქვარცხავა*, ვ. ჟღამაძე*, გ. კახნიაშვილი*

** საქართველოს ტექნიკური უნივერსიტეტი, ვლადიმერ ჭავჭანიძის სახელობის კიბერნეტიკის ინსტიტუტი, თბილისი, საქართველო*
*** ბელარუსის სახელმწიფო ტექნოლოგიური უნივერსიტეტი, ფიზიკური, კოლოიდური და ანალიტიკური ქიმიის დეპარტამენტი, მინსკი, ბელარუსის რესპუბლიკა*

(წარმოდგენილია აკადემიის წევრის თ. ნატრიაშვილის მიერ)

წინამდებარე ნაშრომში წარმოდგენილია $CaMnO_3$ კერამიკის თერმოელექტრულ თვისებებზე Lu_2O_3/Er_2O_3 და $Na_2B_4O_7$–ით თანადოპირების ზეგავლენის კვლევის წინასწარი შედეგები. მიღებული მასალების ფაზური შედგენილობა და მიკროსტრუქტურა შესწავლილ იქნა რენტგენოდიფრაქციული ანალიზისა და მასკანირებელი ელექტრონული მიკროსკოპიის მეთოდების გამოყენებით. კუთრი წინაღობის, ზეებეკის კოეფიციენტისა და თბოგამტარობის გაზომვათა საფუძველზე გამოთვლილია საკვლევი ნიმუშების *PF* და *ZT*–ის მნიშვნელობები. Lu_2O_3 და $Na_2B_4O_7$–ით თანადოპირებამ განაპირობა $CaMnO_3$–ის სისტემის სიმძლავრის ფაქტორის 2–ჯერ და ვარგისობის მაჩვენებლის 4-ჯერ გაუმჯობესება 973 და 573 K ტემპერატურის პირობებში, შესაბამისად. სინთეზის პირობებისა და დოპირების დონის ოპტიმიზაციის შედეგად შესაძლებელია *PF* და *ZT*–ის მნიშვნელობათა შემდგომი ამაღლება.

REFERENCES

1. He J., Liu Y., Funahashi R. (2011) Oxide thermoelectrics: the challenges, progress, and outlook, *Journal of Materials Research*, **26:**1762–1772, DOI: https://doi.org/10.1557/jmr.2011.108.
2. Ankam Bhaskar, Chia-Jyi Liu, J.J. Yuan, Ching-Lin Chang (2013) Thermoelectric properties of n-type $Ca_{1-x}Bi_xMn_{1-y}Si_yO_{3-\delta}$ (x=y=0.00, 0.02, 0.03, 0.04, and 0.05) system, *Journal of Alloys and Compounds,* **552:** 236–239, DOI: https://doi.org/10.1016/j.jallcom.2012.10.078.
3. Terasaki I., Sasago Y., Uchinokura K. (1997) Large thermoelectric power in $NaCo_2O_4$ single crystals, *Physical Review B*, **56:** R12685-R12687, DOI:https://doi.org/10.1103/PhysRevB.56.R12685.
4. Funahashi R., Matsubara I., Ikuta H., Takeuchi T.,Mizutani U., Sodeoka S. (2000) An oxide single crystal with high thermoelectric performance in air, *Jpn. J. Appl. Phys*., **39**: L1127-L1129, DOI:https://doi.org/10.1143/JJAP.39.L1127.
5. Masset A. C., Michel C., Maignan A., Hervieu M., Toulemonde O., Studer F., Raveau B., Hejtmanek J. (2000) Misfit-layered cobaltite with an anisotropic giant magnetoresistance: $Ca_3Co_4O_9$, *Phys. Rev. B*, **62**: 166–175, DOI:https://doi.org/10.1103/PhysRevB.62.166.
6. Tarascon J.M., Ramesh R., Barboux P., Hedge M.S., Hull G.W., Greene L.H., Giroud M., et al. (1989) New non-superconducting layered Bi-Oxide phases of formula $Bi_2M_3Co_2O_y$ containing co instead of Cu, *Solid State Commun*., **71**: 663–668, DOI:https://doi.org/10.1016/0038-1098(89)91813-9.
7. Funahashi R., Matsubara I., Sodeoka S. (2000) Thermoelectric properties of $Bi_2Sr_2Co_2O_x$ polycrystalline materials, *Appl. Phys. Lett*., **76**: 2385–2387, DOI:https://doi.org/10.1063/1.126354.
8. Paredes-Navia S.A, Liang L., Romo-De-La-Cruz C.-O., Gemmen E., Fernandes A., Prucz J., Chen Y., Song X. (2021) Electrical conductivity increase by order of magnitude through controlling sintering to tune hierarchical structure of oxide ceramics, *Journal of Solid State Chemistry*, **294:** Article 121831, DOI: https://doi.org/10.1016/j.jssc.2020.121831.
9. Zheng X.F., Liu C.X., Yan Y.Y., Wang Q. (2014) A review of thermoelectrics research – Recent developments and potentials for sustainable and renewable energy applications, *Renewable and Sustainable Energy Reviews*, **32:** 486–503, DOI:10.1016/j.rser.2013.12.053.
10. Zhou Y.C., Wang C.L., Su W.B., Liu J., Wang H.C., Li J.C., Li Y., Zhai J.Z., Zhang Y.C., Mei L.M. (2016) Electrical properties of Dy^{3+}/Na^+ co-doped oxide thermoelectric $[Ca_{1-x}(Na_{1/2}Dy_{1/2})_{(x)}]MnO3$ ceramics, *Journal of Alloys and Compounds*, **680**: 129-132, https://doi.org/10.1016/j.jallcom.2016.04.158
11. Weishu Liu, Hee Seok Kim, Qing Jie, Zhifeng Ren. (2016) Importance of high power factor in thermoelectric materials for power generation application: A perspective, *Scripta Materialia*, **111:** 3-9, https://doi.org/10.1016/j.scriptamat.2015.07.04.
12. Bhaskar, A., Liu, C.J., Yuan, J. (2012) Thermoelectric and magnetic properties of $Ca_{0.98}RE_{0.02}MnO_{3-\delta}$ (RE = Sm, Gd, and Dy), *J. Electron. Mater*., **41:** 2338–2344, https://doi.org/10.1007/s11664-012-2159-6.
13. Bresch S., Mieller B., Moos R., Torsten R. (2022) Lowering the sintering temperature of calcium manganate for thermoelectric applications, *AIP Advances*, **12:** 085116, https://doi.org/10.1063/5.0098015.
14. Kohri H., Kato M., Ohsugi Isao J., Ichiro Shiota I. (2010) Thermoelectric generating properties of perovskite like materials, *Advances in Science and Technology*, **74:** 72-76, doi:10.4028/www.scientific.net/AST.74.72.
15. Nag A. (2023) Perovskite oxide thermoelectric module - a way forward, *Catalysis Research*, **3**: 024; doi:10.21926/cr.2304024.
16. Madre Maria A., Amaveda H., Dura Oscar J., Pelloquin D., Mora M., Torres Miguel A., Marinel S., Sotelo A. (2023) Effect of Y, La, and Yb simultaneous doping on the thermal conductivity and thermoelectric performances of $CaMnO_3$ ceramics, *Journal of Alloys and Compounds*, **954:** article 170201, https://doi.org/10.1016/j.jallcom.2023.170201.
17. Ohtaki M., Hisako K., Tokunaga T., Eguchi K., Arai H. (1995) Electrical transport properties and high-temperature thermoelectric performance of $(Ca_{0.9}M_{0.1})MnO_3$ (M = Y, La, Ce, Sm, In, Sn, Sb, Pb, Bi), *Journal of Solid State Chemistry*, **120:** 105-111, https://doi.org/10.1006/jssc.1995.1384.
18. Ogawa R., Fujihara S., Hagiwara M. (2022) Effect of dual doping by rare-earth and sodium ions on thermoelectric properties of $CaMnO_3$ ceramics, *Journal of the Ceramic Society of Japan*, **137:** 403-409, DOI: https://doi.org/10.2109/jcersj2.21191.
19. Zhan B., Lan J., Liu Y., Lin Y., Shen Y., Nan C. (2014) High temperature thermoelectric properties of Dy-doped $CaMnO_3$ Ceramics, *Journal of Materials Science & Technology*, **30:** 821-825, DOI: https://doi.org/10.1016/j.jmst.2014.01.002.
20. Vijay A., Charan Prasanth S., Roshan J., Venkata S. K. (2023) Enhancement in the electrical transport properties of $CaMnO_3$ via La/Dy co-doping for improved thermoelectric performance, *RSC Advances*, **13:** 19651-19660, DOI: http://dx.doi.org/10.1039/D3RA03053A.
21. Yuan-Hu Zhu, Wen-Bin Su, Jian Liu, Yu-Cheng Zhou, Jichao Li, Xinhua Zhang, Yanling Du, Chun-Lei Wang. (2015) Effects of Dy and Yb co-doping on thermoelectric properties of CaMnO3 ceramics, *Ceramics International*, **41**: 1535-1539, DOI: https://doi.org/10.1016/j.ceramint.2014.09.089.
22. Yang Wang, Yu Sui, Wenhui Su. (2008) High temperature thermoelectric characteristics of $Ca_{0.9}R_{0.1}MnO_3$ (R=La,Pr, . . . ,Yb), *Journal of Applied Physics*, **104**, 093703, http://dx.doi.org/10.1063/1.3003065.

23. Rapaka S. C. Bose, Nag A. (2018) Investigation of thermoelectric performance and power generation characteristics of dual-doped $Ca_{1-x}RE'_x/2RE''_x/2MnO_3$ (RE′/RE″ = Dy, Gd, Yb, Lu; $0.05 \le x \le 0.1$), *ACS Applied Energy Materials,* **1:** 3151–3158, https://doi.org/10.1021/acsaem.8b00368.
24. Löhnert R., Stelter M., Töpfer J. (2017) Evaluation of soft chemistry methods to synthesize Gd-doped $CaMnO_{3-\delta}$ with improved thermoelectric properties, *Materials Science and Engineering: B*, **223:** 185-193, DOI:10.1016/j.mseb.2017.06.014.
25. Yamashita T. (2007) Physical properties of Na doped CaMnO3, *Materials Chemistry and Physics*, **103:** 461-464, https://doi.org/10.1016/j.matchemphys.2007.02.054.
26. Khanahmadzadeh S., khojasteh H., Mikaeili N., Hasanpour S. (2017) Facile synthesis of $CaMn_2O_4$ nanoparticles and investigation of photocatalytic activity, optical and magnetic properties and its influence on the thermal stability of polymeric nanocomposite*, J. Mater Sci: Mater. Electron*., **28:** 4521–4529, https://doi.org/10.1007/s10854-016-6087-8.
27. Shannon R.D. (1976) Revised effective ionic radii and systematic studies of interatomic distances in halides and chalcogenides, *Acta Crystallographica A*, **32:** 751-767, https://doi.org/10.1107/S0567739476001551.
28. Torres, Samanta de O. A., Thomazini D., Balthazar, Gabriel P., Gelfuso, Maria V. (2020) Microstructural influence on thermoelectric properties of CaMnO3 ceramics, *Materials Research*, **23:** e20200169, https://doi.org/10.1590/1980-5373-MR-2020-0169.
29. Mouyane M., Itaalit B., Bernard, J., Houivet D., Noudem Jacques G. (2014) Flash combustion synthesis of electron doped-$CaMnO_3$ thermoelectric oxides, *Powder Technology*, **264:** 71-77, https://doi.org/10.1016/j.powtec.2014.05.022.
30. Xu G., Funahashi R., Qirong P., Liu B., Tao R., Wang G., Zejun Ding Z. (2004) High-temperature transport properties of Nb and Ta substituted $CaMnO_3$ system, *Solid State Ionics*, **171:**147–151, https://doi.org/10.1016/S0167-2738(03)00108-5.

Received December, 2023